Hindawi Publishing Corporation
Advances in Optical Technologies
Volume 2008, Article ID 383927, 6 pages
doi:10.1155/2008/383927

Research Article

Silicon Photonic Biosensors for Lab-on-a-Chip Applications

Kirill Zinoviev,[1] Laura G. Carrascosa,[2] José Sánchez del Río,[2] Borja Sepúlveda,[2] Carlos Domínguez,[1] and Laura M. Lechuga[2]

[1] *Instituto de Microelectronica de Barcelona, CNM-CSIC, Campus UAB, Bellaterra 08193, Barcelona, Spain*
[2] *Nanobiosensors and Molecular Nanobiophysics Group, Research Center on Nanoscience and Nanotechnology (CIN2: CSIC-ICN), Campus UAB, Bellaterra 08193, Barcelona, Spain*

Correspondence should be addressed to Laura M. Lechuga, laura.lechuga@cin2.es

Received 13 February 2008; Accepted 24 April 2008

Recommended by Pavel Cheben

In the last two decades, we have witnessed a remarkable progress in the development of biosensor devices and their application in areas such as environmental monitoring, biotechnology, medical diagnostics, drug screening, food safety, and security, among others. The technology of optical biosensors has reached a high degree of maturity and several commercial products are on the market. But problems of stability, sensitivity, and size have prevented the general use of optical biosensors for real field applications. Integrated photonic biosensors based on silicon technology could solve such drawbacks, offering early diagnostic tools with better sensitivity, specificity, and reliability, which could improve the effectiveness of in-vivo and in-vitro diagnostics. Our last developments in silicon photonic biosensors will be showed, mainly related to the development of portable and highly sensitive integrated photonic sensing platforms.

Copyright © 2008 Kirill Zinoviev et al. This is an open access article distributed under the Creative Commons Attribution License, which permits unrestricted use, distribution, and reproduction in any medium, provided the original work is properly cited.

1. INTRODUCTION

The progressive demand for the rapid and precise detection of any type of substances has speed up the development of a large variety of biosensors. For most of the applications, it is desirable to have a compact biosensor with high sensitivity, fast response, and able to perform real-time measurements. These requirements can be achieved mainly with optical sensors [1] due to the own nature of the optical measurements that endow a great number of different techniques, as emission, absorption, fluorescence, refractometry, or polarimetry. Among them, photonic biosensors based on evanescent wave detection have demonstrated its outstanding properties, such as an extremely high sensitivity for the direct measurement of biomolecular interactions, in real time and in label-free schemes [1].

In the evanescent wave detection, a receptor layer is immobilized onto the core surface of the waveguide. The exposure of the functionalized surface to the complementary analyte molecules and the subsequent biochemical interaction between them induces a local change in the optical properties of the biological layer. This change is detected via the evanescent field of the guided light and its amplitude can be correlated to the concentration of the analyte and to the affinity constant of the interaction, yielding a quantitative signal of the interaction.

The wide variety of optical sensing platforms is spread over sensors based on optical fibers [2], planar waveguide structures [3], microresonators [4–6], resonant waveguide diffractive structures [7, 8], light addressable potentiometric devices (LAPS) [9, 10], micromechanical structures with optical readout [11], porous silicon [12, 13], and so forth.

The advantages of optical sensing are significantly improved when this approach is used within an integrated optics context. Integrated optics technology allows the integration of passive and active optical components (including fibres, emitters, detectors, waveguides, and related devices) onto the same substrate, allowing the flexible development of miniaturized compact sensing devices, with the additional possibility to fabricate multiple sensors on a single chip. The integration offers additional advantages such as miniaturization, robustness, reliability, potential for mass production with consequent reduction of production costs, low energy consumption, and simplicity in the alignment of the individual optical elements.

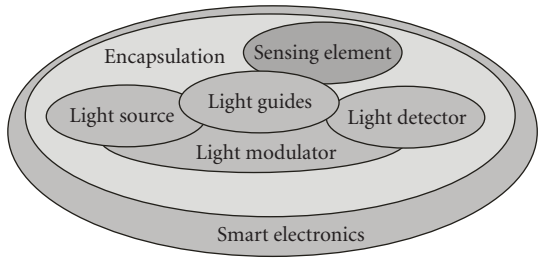

Figure 1: The main research areas in the development of photonics biosensors based on silicon technology.

Several technologies are available for the fabrication of photonic biosensors, but the well-developed silicon technology is one of the most useful and promising tools. Much work on silicon photonic devices has been done in the telecommunications field, and some results have been successfully applied for sensor development. In "siliconized" photonics, the fabrication of the devices is performed with silicon or silicon-related materials using microelectronics technologies, with the aim of integrating all the sensing components in a single chip. In order to "siliconize" photonics, there are several building blocks for investigation, including light generation and coupling, selectively guiding and transporting within the waveguides, light encoding, detection, packaging the devices, and, finally, "smart" electronic control of all these photonic functions (see Figure 1). Biofunctionalization of the sensing element is a subject of special research beyond photonics, thus the element has been highlighted in a separate block on the diagram of Figure 1.

In particular, light guiding for sensing applications can be based on total internal reflection (TIR) planar or rib waveguides [3, 14, 15], hollow waveguides [16–19], antiresonant reflecting optical waveguides (ARROW) [20–22], or slot [4, 23] waveguides. Interestingly, complex waveguide structures developed for telecommunications with the purpose of further miniaturization of photonics devices, which show potential sensing applications, have been reported recently [24].

In this paper, we will discuss the photonic biosensing platforms based on silicon technology, which are investigating in our laboratory, such as interferometric Mach-Zehnder (MZI), bimodal waveguides devices, and optomechanical microcantilevers. The three devices have advantages and disadvantages and depending on the specific biological application one is more suitable than the others. The interferometric MZI sensors show extremely high sensitivity; however, the existing light coupling methods frequently limit their application to laboratory use only. High thermal stability is required for the bimodal waveguide interferometers but this device is simpler in operation than the MZI. The optical microcantilevers also require a high mechanical and thermal stability for operation but this device is easily scalable to dozens or hundreds of sensors in the same chip opening the way to high-throughput screening using label-free biosensors. The main aim of this article is to describe the use of silicon technology for the implementation of integrated optical biosensor rather than to perform a sensitivity comparison between the different devices.

2. INTEGRATED MACH-ZEHNDER INTERFEROMETER (MZI) SENSOR

Interferometric biosensors constitute one of the most sensitive integrated-optic alternatives as compared to other optical biosensor (i.e., plasmonic biosensors) for label-free detection. In these sensors, the guided light interacts with the analyte through its evanescent field or, alternatively, the analyte can propagate in the core of the waveguide if hollow or slot waveguides are employed. The most common Mach-Zehnder and Young interferometers [3, 25, 26] are composed of an incident waveguide that is split in two single mode waveguide branches, in which one of them contains a sensing window.

We have developed integrated Mach-Zehnder interferometers based on TIR waveguides ($Si/SiO_2/Si_3N_4$) of micro/nanodimensions, as it is shown on Figure 2. For biosensing applications, the optical waveguides of the MZI must have high surface sensitivity and single mode behavior. For that reason, we have chosen Si_3N_4 core layers ($n_c = 2.00$) over a SiO_2 substrate ($n_s = 1.46$). In this waveguide configuration (and wavelength in the visible range), the single mode behavior is obtained for core thickness below 300 nm. In order to provide single mode operation in the lateral direction, rib structures several nanometers high (below 5 nm) and rib widths of 4 μm were fabricated. To achieve single mode behavior, the waveguide could be designed to be narrower and with a higher rib but this will depend on the tolerances of the equipment available for the fabrication. With the equipment of our facilities, we can ensure the reproducibility of the rib height at a nanometric scale which allows us to make relatively wide waveguides which are more convenient for experimental work. Figure 2 shows a schematic of the waveguide configuration. In the MZI, Y-shape divisors with circular arms of $R = 80$ mm were designed to direct light in the two branches of the MZI with 3 dB split ratio. To protect the device from temperature fluctuations, the waveguide branches are placed very close to each other (100 μm,), thus the temperature changes affect both waveguides simultaneously.

The devices are fabricated in our clean room facilities. The final device has a length of 3 cm and the sensor area is 1.5 cm long and 50 μm wide. The experimental evaluation of the device was performed in an optical bench, where polarized light from an He-Ne laser ($\lambda = 0{\cdot}633\,\mu$m) was end-fire coupled to the sensor. The propagation losses of the waveguides were measured by the Fabry-Perot resonance technique, and the optical coupling losses were measured by the cutback method. Propagation losses, in the case of MZI of 200 nm core thickness, vary between 0.13 and 0.15 dB/cm for TE polarization and between 0.27 and 0.30 dB/cm for TM polarization. Insertion losses are 5.84 dB for TM polarization and 8.3 dB for TE polarization. The sensitivity of the sensor for both polarizations was analyzed in the same way as in previous reports [3]. The evaluation was done flowing solutions of water and ethanol of varying concentration

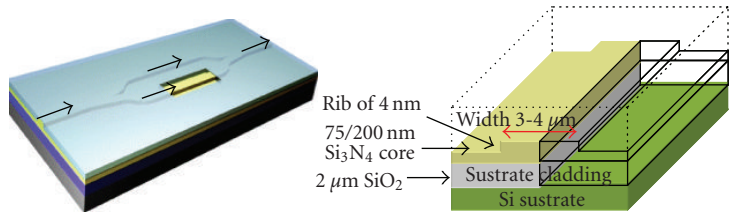

FIGURE 2: (left). Mach-Zehnder interferometer (MZI) configuration. (right) Cross-section schematic of the TIR waveguides employed in the integrated MZI device.

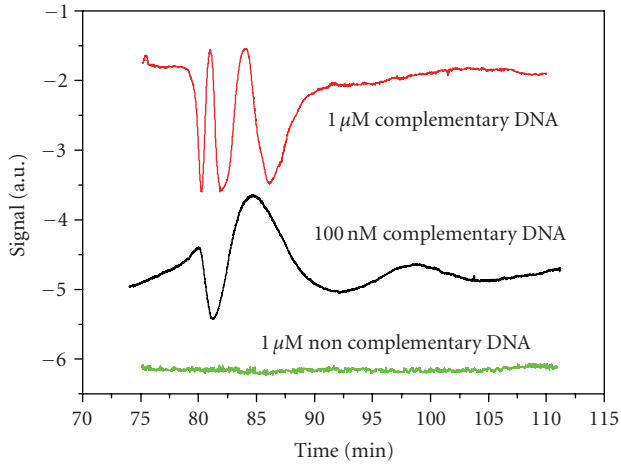

FIGURE 3: Real-time DNA hybridization signal corresponding to 1 μM and 100 nM complementary oligonucleotide and 1 μM noncomplementary oligonucleotide.

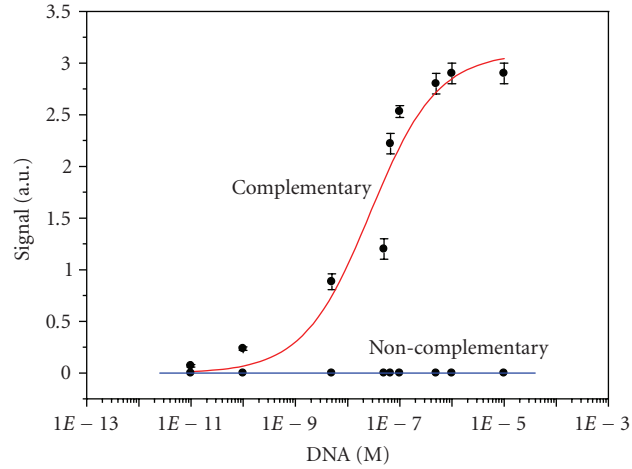

FIGURE 4: Calibration curve for the hybridization of complementary (red line) and noncomplementary (blue line) DNA (58 mers). Limit of detection is 10 pM.

(refractive index steps of 10^{-3}) and measuring the output signal in real time. Taking into account the signal-to-noise ratio of our system, the lowest detection limit in the variation of the refractive index (n_0) for the TM polarization was found to be $\Delta n_{0,\min} = 1 \cdot 10^{-7}$.

The relatively simple design, high integration level, well developed read out techniques, and the high sensitivity make these devices very attractive for bio/chemical applications. The MZI device has been used for the direct detection of DNA hybridization and for the detection of single mutations at the BRCA-1 gene, involved in breast cancer development, without target labelling [27]. The oligonucleotide probe is immobilized by covalent attachment to the sensor surface through silanization procedures. A silane (3-mercaptopropyltrimethoxysilane) with a thiol group at the free end was employed for the chemical modification of the surface. A thiol-derivatized oligonucleotides (28 mer) used as receptors can bind to the silanized Si_3N_4 surface through a disulphide bond. The DNA probe has also a 15-tiamine tail which is employed as a vertical spacer chain to increase the accessibility to the complementary DNA to the sensor surface.

After DNA immobilization, complementary oligonucleotides (58 mer) were flowed in the sensor for hybridization experiments. The hybridization was performed for different DNA target concentrations from 1 pM to 1 μM. Regeneration after each hybridization was achieved flowing deionized water and HCl 3.2 mM. Figure 3 shows examples of the real-time detection of DNA hybridization for several concentrations. The calibration curve as a function of the DNA concentration can be seen in Figure 4. In these measurements, a 10 pM-concentration of complementary nonlabelled DNA in buffer solution was the lowest hybridization limit achieved, which means an average DNA growth layer of $1 \cdot 14^{-4}$ nm, corresponding to an estimation of $2 \cdot 10^5$ DNA molecules/cm^2 hybridized at the sensor area of the MZI. In contrast, noncomplementary oligonucleotides did not show any significant signal.

More importantly, we have detected the hybridization of 100 nM DNA target with two mismatching bases corresponding to a mutation of the BRCA-1 gene (data not shown). These results place the Mach-Zehnder interferometer as one of the most sensitive optical biosensor for label-free mismatch and DNA hybridisation detection.

3. BIMODAL WAVEGUIDE SENSOR

This sensor is comprised by a single straight bimodal waveguide (BiMW), which supports the zero- and first-order transversal modes (see Figure 5). These modes propagate with different velocities depending, among other factors, on the refractive index of the cladding layer. The interference

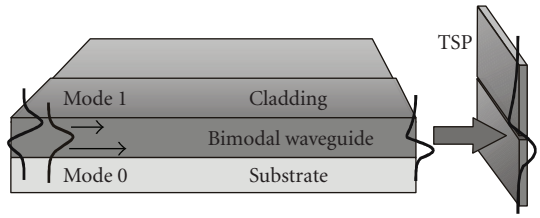

Figure 5: Schematic view of the bimodal waveguide sensor device. The modes are propagating with different velocities. The interference pattern, created at the exit and projected onto a two-sectional photodetector (TSP), varies as a function of the refractive index of the cladding layer.

pattern formed at the exit of the waveguide changes if the refractive index varies. The pattern is projected on a two-sectional photodetector (TSP), then the intensity maximum moves between the lower and the upper sections of the photodetector. The signals generated by the photodetector sections are recalculated into a parameter S_r, according to the expression

$$S_r = \frac{U_{\text{up}} - U_{\text{down}}}{U_{\text{up}} + U_{\text{down}}}, \tag{1}$$

where U_{up}, U_{down} are the signals generated by the upper and the lower sections of the photodetector, respectively.

The difference between U_{up}, and U_{down} can reach 17 dB, which means a variation of S_r from 0 to 0.96. These values were calculated assuming a silicon nitride waveguide with thickness of 400 nm operated at 633 nm. The total output signal, which can be represented by the denominator in the right part in (1), is proportional to the light power coupled into the waveguide, except for minor changes due to reflection at the output facet, which slightly depends on the intensity distribution at the exit, according to the simulations. Using the parameter S_r, the ambiguities due to coupling efficiency variations can be significantly reduced. However, as the monitoring of light power coupled into the waveguide is still desirable, a part of the incoupled light can be tapped off and measured with a conventional photodetector. The sensitivity of the device is given by

$$\text{Sens} = \frac{\partial S_r}{\partial \phi}\left(\frac{\partial n_{\text{eff}}^1}{\partial n_{\text{cl}}} - \frac{\partial n_{\text{eff}}^0}{\partial n_{\text{cl}}}\right)\frac{2\pi}{\lambda}L, \tag{2}$$

where L is the length of the sensing window, λ is the wavelength, n_{eff}^0, n_{eff}^1 are the effective refractive index of the zero- and first-order modes, respectively, φ is the phase shift between the modes, and n_{cl} is the refractive index of the cladding layer.

For the experiments, we employed a 3 μm-wide, 400 nm thick Si_3N_4 waveguide deposited on a silicon dioxide buffer layer, and the length of the sensing area was 3 mm. The waveguide was excited by direct focusing of light from an He-Ne laser (633 nm, 10 mW). A slight misalignment of the objective with respect to the waveguide in the vertical direction allows for excitation of both modes simultaneously. Light was collected by an objective lens, and the image of the waveguide facet was projected on the photodetector (TSP).

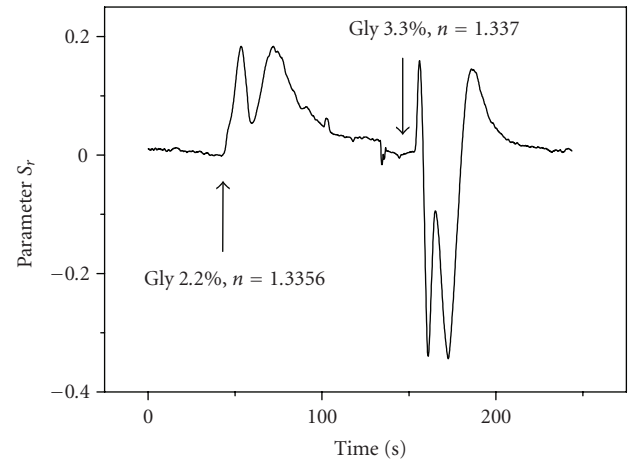

Figure 6: Response of the BiMW sensor to the injection of glycerin solutions with concentrations of 2.2% and 3.3% (v).

The detection of the refractive index changes was performed by injecting varying concentrations of water/glycerin solutions into a microfluidic channel formed over the sensing area. An example of the changes of the interferogram due to refractive index variation is shown in Figure 6. The sensitivity, defined as the relative change in the output signal per RIU change, can reach a value of better than 1×10^4 per RIU on a 1 cm-long waveguide with thickness less than 400 nm. A sensitivity of 2×10^3 per RIU was demonstrated experimentally on a silicon nitride waveguide with thickness of 400 nm. The obtained sensitivity was limited mostly by the thickness of the waveguide and by the coupling technique which allowed for only 25% modulation of the output signal. Biosensing experiments with this device are in progress.

4. OPTICAL MICROCANTILEVER BIOSENSOR

The development of microprobes for atomic force microscopy (AFM) was an important milestone for the establishment of efficient technological approaches to MEMS sensors. The principle of operation of the microcantilever sensor is based on the bending induced in the cantilever when a biomolecular interaction takes place in one of its surfaces. In this way, microcantilevers translate the molecular reaction into a nanomechanical motion, which is commonly detected using optical or piezoresistive readout [28].

In order to achieve highly integrated microsystem with microcantilever transducers, we have recently introduced a new type of readout technique. The combination of photonics and mechanics has been demonstrated in an optical waveguide cantilever sensor. The sensor can work in static or dynamic modes, either by monitoring the deflection or the changes in the resonance frequency of the cantilever. The principle of operation is based on the sensitivity of energy transfer between two butt-coupled waveguides to their misalignment with respect to each other as it is represented in Figure 7. The advantage of the device is that the transducer is integrated with the receptor in the same chip and the external photodetector is only used for optical

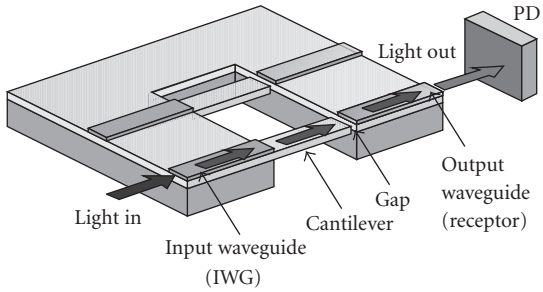

Figure 7: Sketch of the sensor based on optical waveguide microcantilevers.

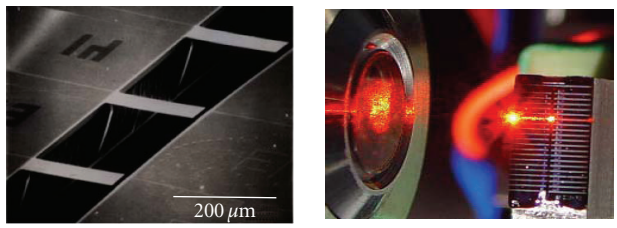

Figure 8: Photographs of the optical cantilevers and the light coupling inside them.

power readout. No preliminary alignment or adjustment is needed, except for light coupling into the chip.

We have fabricated arrays of 20 optical microcantilevers. Each of them is 200 μm long, 40 μm wide, and 500 nm thick with a spring constant of 0.050 N/m. Fabrication of the sensor is done using standard microelectronic technology. The cantilevers are made of thermal silicon dioxide, transparent in visible range. Input and output waveguides are made of silicon nitride and are 140 nm-thick and 40 μm-wide. The cantilever has low stress gradient and is practically flat, the misalignment between the output waveguide and the cantilever free end is around 1 μm. Some photographs of the fabricated devices can be seen in Figure 8. Coupling of the light in the cantilever is achieved through the evanescent field of the input waveguide.

In order to characterize the sensor, an experimental setup was used to measure the amplitude of modulation of the output signal induced by the vibration of the cantilever at the resonance frequency. Light from He-Ne laser (632.8 nm, 7.5 mW) was coupled into the chip using direct focusing with an objective lens (40x, NA 0.65) and was collected upon exiting by another objective (40x, NA 0.65) before being directed to a silicon photodetector connected to an oscilloscope and an acquisition system for spectrum analysis through a low-noise amplifier with bandwidth 5 to 45 kHz, at FWHM. Light from the same laser source after splitting was focused by a lens with a focal distance of 75 mm on the cantilever near its free end. The reflected beam was projected on to a two-sectional position sensitive photodetector to monitor the displacement of the cantilever. Clear resonance behavior near 13 kHz with a Q-factor of 12 was observed [11]. The change in the output voltage per unit cantilever displacement was calculated to be 15 μV/nm, thus nanometre resolution of the system was demonstrated.

Taking account in this configuration that the minimum detectable deflection is limited by the shot noise of the photodetector, the Johnson noise of the load resistor, the noise in the acquisition system, the cantilever vibration due to the thermal noise, and the noise produced by the laser source, we have estimated that, for a 1 μm wide gap, the cantilever displacement can be detected with a resolution of 18 fm/$\sqrt{\text{Hz}}$ [11], showing similar performances for biosensing than the standard microcantilevers.

One of the advantages of this device is that real-time parallel monitoring of several channels can be done simultaneously, opening the way for multisensing. The cantilever can be metallized with gold (and then it is possible to use the well-known thiol chemistry for bioreceptors immobilization) and its initial displacement can be adjusted by varying the power of light coupled inside [29]. This new device has shown good performances for biosensing and offers an interesting approach for further integration in lab-on-a-chip microsystems. The integration with the light source and the biofunctionalization of the device is a subject of our current research.

5. INTEGRATION IN "LAB-ON-A-CHIP" MICROSYSTEMS

For the development of a complete photonic lab-on-a-chip microsystem device, several units must be incorporated on the same platform: (i) the micro/nanodevices, (ii) the flow cells and the flow delivery system, (iii) for interferometric sensors, a phase modulation system to convert the periodic output signal in direct phase measurements, (iv) integration of the light sources and the photodetectors, and (v) CMOS processing electronics. For achieving this goal, our first step has been the development of a novel low temperature (100°C) CMOS compatible microfluidic technology to create 3D embedded interconnected microfluidic channels between different substrates. The microfluidic channels have a height from 40 to 60 μm and a width between 100 to 250 μm. More details can be found in [30].

6. CONCLUSIONS

We have presented the development of different integrated optical biosensor platforms based on silicon technologies: a Mach-Zehnder integrated interferometer, a bimodal waveguide sensor, and a waveguided microcantilever device. The feasibility of the different platforms for biosensing has been proved. In the case of the MZI device, we have achieved a lowest limit of detection of 10 pM for the DNA hybridization of the BRCA-1 gene, involved in breast cancer development. These results place the Mach-Zehnder interferometer as one of the most sensitive optical biosensor for label-free DNA detection.

All the described sensing configurations look ahead the possibility of the integration of optic, fluidic, and electrical functions on one platform to obtain lab-on-a-chip microsystems. These results open the way for further

development of portable and multianalyte sensors for the detection of several biological molecules of interest in situ and in real-time.

ACKNOWLEDGMENTS

Authors would like to thank the financial support of the Spanish Ministry of Education and Science (project TEC2005-13604) and M. Botín Foundation.

REFERENCES

[1] L. M. Lechuga, "Optical biosensors," in *Biosensors and Modern Biospecific Analytical Techniques*, L. Gorton, Ed., vol. 44 of *Comprehensive Analytical Chemistry Series*, pp. 209–250, Elsevier Science BV, Amsterdam, The Netherlands, 2005.

[2] B. Culshaw, "Optical fiber sensor technologies: opportunities and-perhaps-pitfalls," *Journal of Lightwave Technology*, vol. 22, no. 1, pp. 39–50, 2004.

[3] F. Prieto, B. Sepúlveda, A. Calle, et al., "An integrated optical interferometric nanodevice based on silicon technology for biosensor applications," *Nanotechnology*, vol. 14, no. 8, pp. 907–912, 2003.

[4] C. A. Barrios, "Ultrasensitive nanomechanical photonic sensor based on horizontal slot-waveguide resonator," *IEEE Photonics Technology Letters*, vol. 18, no. 22, pp. 2419–2421, 2006.

[5] T. M. Benson, S. V. Boriskina, P. Sewell, A. Vukovic, S. C. Greedy, and A. I. Nosich, "Micro-optical resonators for microlasers and integrated optoelectronics: recent advances and future challenges," in *Frontiers of Planar Lightwave Circuit Technology: Design, Simulation and Fabrication*, S. Janz, J. Ctyroky, and S. Tanev, Eds., pp. 39–70, Springer, Berlin, Germany, 2005.

[6] H.-C. Ren, F. Vollmer, S. Arnold, and A. Libchaber, "High-Q microsphere biosensor-analysis for adsorption of rodlike bacteria," *Optics Express*, vol. 15, no. 25, pp. 17410–17423, 2007.

[7] Y. Fang, A. M. Ferrie, N. H. Fontaine, J. Mauro, and J. Balakrishnan, "Resonant waveguide grating biosensor for living cell sensing," *Biophysical Journal*, vol. 91, no. 5, pp. 1925–1940, 2006.

[8] M. Wiki, R. E. Kunz, G. Voirin, K. Tiefenthaler, and A. Bernard, "Novel integrated optical sensor based on a grating coupler triplet," *Biosensors & Bioelectronics*, vol. 13, no. 11, pp. 1181–1185, 1998.

[9] D. G. Hafeman, J. W. Parce, and H. M. McConnell, "Light-addressable potentiometric sensor for biochemical systems," *Science*, vol. 240, no. 4856, pp. 1182–1185, 1988.

[10] W. J. Parak, M. George, J. Domke, et al., "Can the light-addressable potentiometric sensor (LAPS) detect extracellular potentials of cardiac myocytes?" *IEEE Transactions on Biomedical Engineering*, vol. 47, no. 8, pp. 1106–1113, 2000.

[11] K. Zinoviev, C. Domínguez, J. A. Plaza, V. J. C. Busto, and L. M. Lechuga, "A novel optical waveguide microcantilever sensor for the detection of nanomechanical forces," *Journal of Lightwave Technology*, vol. 24, no. 5, pp. 2132–2138, 2006.

[12] L. De Stefano, P. Arcari, A. Lamberti, et al., "DNA optical detection based on porous silicon technology: from biosensors to biochips," *Sensors*, vol. 7, no. 2, pp. 214–221, 2007.

[13] J. J. Saarinen, S. M. Weiss, P. M. Fauchet, and J. E. Sipe, "Optical sensor based on resonant porous silicon structures," *Optics Express*, vol. 13, no. 10, pp. 3754–3764, 2005.

[14] A. Densmore, D.-X. Xu, S. Janz, et al., "Spiral-path high-sensitivity silicon photonic wire molecular sensor with temperature-independent response," *Optics Letters*, vol. 33, no. 6, pp. 596–598, 2008.

[15] B. J. Luff, J. S. Wilkinson, J. Piehler, U. Hollenbach, J. Ingenhoff, and N. Fabricius, "Integrated optical Mach-Zehnder biosensor," *Journal of Lightwave Technology*, vol. 16, no. 4, pp. 583–592, 1998.

[16] V. J. Cadarso, I. Salinas, A. ALlobera, and C. Domínguez, "Multimode interference devices based on silicon," in *Integrated Optics: Theory and Applications*, vol. 5956 of *Proceedings of SPIE*, pp. 1–8, Warsaw, Poland, August 2005.

[17] R. Bernini, S. Campopiano, L. Zeni, and P. M. Sarro, "ARROW optical waveguides based sensors," *Sensors and Actuators B*, vol. 100, no. 1-2, pp. 143–146, 2004.

[18] S. Campopiano, R. Bernini, L. Zeni, and P. M. Sarro, "Microfluidic sensor based on integrated optical hollow waveguides," *Optics Letters*, vol. 29, no. 16, pp. 1894–1896, 2004.

[19] D. Yin, J. P. Barber, E. Lunt, et al., "Planar single-molecule sensors based on hollow-core ARROW waveguides," in *Silicon Photonics*, vol. 6125 of *Proceedings of SPIE*, pp. 1–13, San Jose, Calif, USA, January 2006.

[20] F. Prieto, A. Llobera, D. Jiménez, A. Calle, C. Domínguez, and L. M. Lechuga, "Design and analysis of silicon antiresonant reflecting optical waveguides for highly sensitive sensors," *Journal of Lightwave Technology*, vol. 18, no. 7, pp. 966–972, 2000.

[21] F. Prieto, L. M. Lechuga, A. Calle, A. Llobera, and C. Domínguez, "Optimised silicon antiresonant reflecting optical waveguides for sensing applications," *Journal of Lightwave Technology*, vol. 19, no. 1, pp. 75–83, 2001.

[22] A. Llobera, J. A. Plaza, I. Salinas, et al., "Technological aspects on the fabrication of silicon-based optical accelerometer with ARROW structures," *Sensors and Actuators A*, vol. 110, no. 1–3, pp. 395–400, 2004.

[23] T. Fujisawa and M. Koshiba, "Guided modes of nonlinear slot waveguides," *IEEE Photonics Technology Letters*, vol. 18, no. 14, pp. 1530–1532, 2006.

[24] S. V. Boriskina, "Spectral engineering of bends and branches in microdisk coupled-resonator optical waveguides," *Optics Express*, vol. 15, no. 25, pp. 17371–17379, 2007.

[25] A. Ymeti, J. S. Kanger, R. Wijn, P. V. Lambeck, and J. Greve, "Development of a multichannel integrated interferometer immunosensor," *Sensors and Actuators B*, vol. 83, no. 1–3, pp. 1–7, 2002.

[26] A. Densmore, D.-X. Xu, P. Waldron, et al., "A silicon-on-insulator photonic wire based evanescent field sensor," *IEEE Photonics Technology Letters*, vol. 18, no. 23, pp. 2520–2522, 2006.

[27] B. Sepúlveda, J. Sánchez del Río, M. Moreno, et al., "Optical biosensor microsystems based on the integration of highly sensitive Mach-Zehnder interferometer devices," *Journal of Optics A*, vol. 8, no. 7, pp. S561–S566, 2006.

[28] L. G. Carrascosa, M. Moreno, M. Álvarez, and L. M. Lechuga, "Nanomechanical biosensors: a new sensing tool," *Trends in Analytical Chemistry*, vol. 25, no. 3, pp. 196–206, 2006.

[29] K. Zinoviev, C. Domínguez, J. A. Plaza, and L. M. Lechuga, "Optical waveguide cantilever actuated by light," *Applied Physics Letters*, vol. 92, no. 1, Article ID 011908, 3 pages, 2008.

[30] F. J. Blanco, M. Agirregabiria, J. Berganzo, et al., "Microfluidic-optical integrated CMOS compatible devices for label-free biochemical sensing," *Journal of Micromechanics and Microengineering*, vol. 16, no. 5, pp. 1006–1016, 2006.

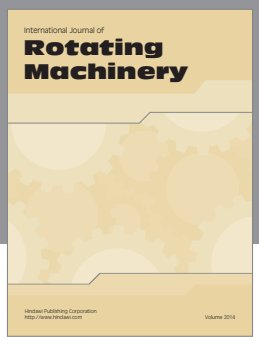

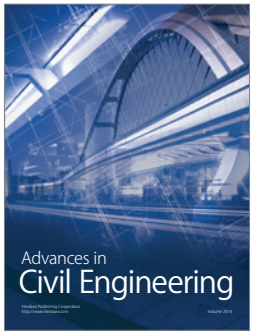

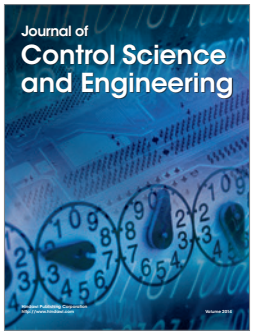

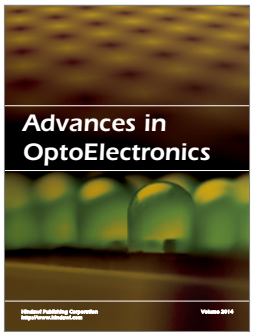

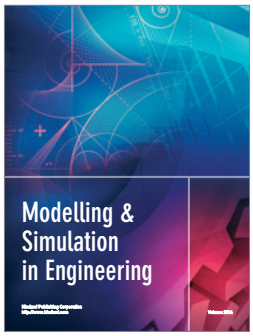

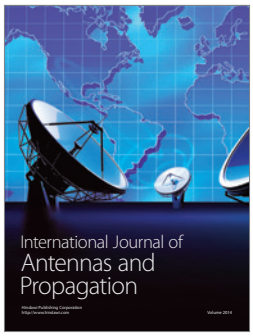

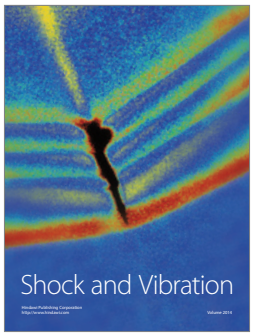

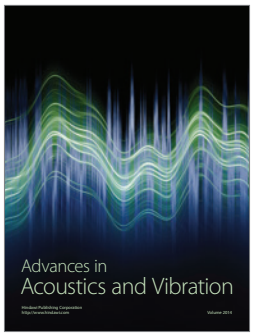

Hindawi

Submit your manuscripts at
http://www.hindawi.com